MOEM

Research Article

Photoluminescences properties of lanthanum-silver co-doped ZnO nano particles

V. Porkalai[1], B. Sathya[1], D. Benny Anburaj[1], G. Nedunchezhian[1],
S. Joshua Gnanamuthu[2], R. Meenambika[3]

1 PG and Research Department of Physics, Thiru.Vi.Ka.Government.Arts College, Thiruvarur, Tamil Nadu-610 003, India

2 PG and Research Department of Physics, TBML College, Porayar Tamil Nadu-609 307, India

3 Marthandam College of Engineering & Technology, Kanyakumari District-629 177, India

Corresponding author: *D. Benny Anburaj* (bennyanburaj@rediffmail.com)

Abstract

Recently, transition metal (TM) and rare earth ion doped II–VI semiconductor nanoparticles have received much attention because such doping can modify and improve optical properties of II–VI semiconductor nanoparticles by large amount. In this study, undoped, La doped and La+Ag co-doped ZnO nano particles have been successfully synthesized by sol-gel method using the mixture of Zinc acetate dihydrate and ethanol solution. The powders were calcinated at 600 °C for 2 h. The effect of lanthanum and lanthanum-silver incorporation on the structure, morphology, optical and electrical conductivity were examined by X-ray diffraction (XRD), Scanning Electron Microscope (SEM), Energy Dispersive X-ray Absorption (EDAX), Fourier transform infrared spectroscopy (FTIR), UV and Photo Luminescence (PL) Characterization. The average particle size of the synthesized ZnO nanoparticles is calculated using the Scherrer formula and is found to be of less than 20 nm. Luminescences properties were found to be enhanced for the La and La+Ag co-doped ZnO nanoparticles.

Keywords

1. Introduction

With great to manipulate structure of the materials on the level of individual atoms and molecules, nanotechnology is a promising highly interdisciplinary field. Nanoparticles can contribute to stronger, lighter, cleaner and smarter surfaces and systems. Transition metal **(TM)** doped ZnO nanoparticles are promising candidates for a variety of practical applications due to their potential applications because such doping can modify and improve optical and electrical properties of these materials. [1–5]. ZnO is one of the most promising materials for short- wavelength optoelectronic applications due to its direct wide band gap of 3.37 eV large bond strength, and large exciton binding energy (60 meV). The missing absorbance of visible light makes this material one of the best transition metal oxide nanoparicles so far [6]. Doping with transition metal oxides leads to many interesting properties of ZnO. With the use of different dopants it is possible to increase or decrease the band gap. After do-

ping, conductivity of ZnO often increases. The effect of dopant element completely depends on its difference between ionic radius of zinc and the dopant material [7, 8].

In this work we report an investigation of structural, optical and electrical properties of pure ZnO, La doped ZnO and La+Ag co-doped ZnO nanoparticles. The sol-gel method was used due to the method being high purity, novel materials, cost effective, which requires low temperatures for processing and a high degree of solubility can be achieved. The structural, morphological optical and electrical properties were investigated using X-ray diffraction **(XRD)**, energy dispersive X-ray **(EDAX)** spectroscopy, Scanning Electron Microscope **(SEM)**, Fourier- transform infrared spectroscopy **(FTIR)**, visible spectrometer **(UV)** and Photo Luminescence **(PL)** Characterization.

2. Experimental procedure

2.1 Synthesis of Zinc Oxide nanoparticles

Pure, La doped and La+Ag co-doped ZnO nanoparticles were synthesized by a simple and low cost sol-gel method. Zinc acetate is taken as the main source for ZnO and is dissolved in distilled water by continuous stirring for half an hour with temperature maintained at 80 °C. Then Lanthanum chloride ($LaCl_3$) and Silver nitrate ($AgNO_3$) taken at appropriate proportion of 0.1M, 0.2M and 0.3M is added drop by drop and mixed thoroughly. To maintain the pH level at 10 and for precipitation, NH_3 and TEA (Triethanolamine) are added respectively. The colloidal precipitate obtained was cooled and washed several times with ethanol and then acetone to remove the organic impurities present, if any. The samples are then kept under microwave irradiation for half an hour till the solvent was evaporated completely. The powders were mixed and grind for 30 min at room temperature and the milled powders were ultimately calcined at 600 °C temperatures for 2 h followed by cooling.

The same procedure is followed to prepare La doped ZnO nanoparticles by using Lanthanum chloride ($LaCl_3$) with the main source Zinc acetate.

2.2 Characterization of the samples

Structural analysis was carried out using X-ray diffractometry **(XRD)** pattometer using CuK_α radiation ($\lambda = 1.5406$ Å) operated at 40 kV and 30 mA in the wide angle region of 2θ range from 30 to 70° with a step size of 0.1°. The morphology and microstructure of the samples were identified by scanning electron microscope (**SEM**, Philip XL 30). The topological features and the composition were determined by energy dispersive X-ray absorption **(EDAX)** using K and L lines respectively. Formation of ZnO wurtzite phase and available molecular bonds were investigated by the FTIR absorption spectrum. The absorbance spectra of the samples were obtained using UV-vis-NIR spectrophotometer to investigate

the optical properties of these nanoparticles,. The spectral absorption spectra were recorded using UV visible spectrometer (model: Lambda 35, make Perkin) in the wave length range 200 to 800 nm using quartz cuvettes at room temperature. The Photoluminescence **(PL)** Spectrum of the ZnO nanoparticles dissolved in methanol has been measured using a spectrophotometer in the range of 400 to 4000 cm^{-1}, (F-2500 FL Spectrophotometer, Hitachi).

3. Results and discussion

3.1. Structural studies

Fig. 1 (*a* and *b*) shows the XRD patterns of pure, La doped and La+Ag co-doped ZnO nanoparticles analysed with Rietveld refinement. The diffraction peaks of the ZnO, ZnO doped with La, and ZnO codoped with La+Ag nanoparticles clearly shows the crystalline nature corresponding to the diffraction planes (100), (002), (101), (111), (102), (110), (200), (103), (112), and (201). The XRD patterns shows the reflection planes indexed wurtzite hexagonal structure of ZnO (space group *P*63*mc*, JCPDF #79-0208 with preferred orientation along (101) plane in all the samples. The refined pattern is in very
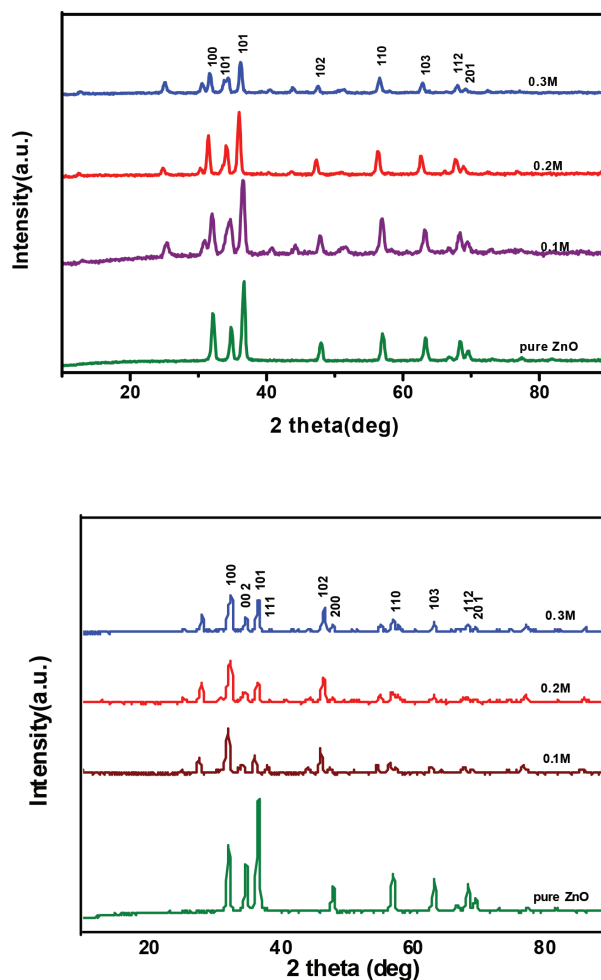
Figure 1. XRD Pattern of pure and (*a*) La doped ZnO nanoparticles, (*b*) La-Ag codoped ZnO nanoparticles.

good agreement with the measured data. No secondary phases such as Oxides of Lanthanum or Oxides of Silver were observed in the samples, as shown in Fig. 1a suggesting that La and Ag occupy the zinc sites in the doped and co-doped ZnO samples. Also it reveals that the substitution of La and La+Ag does not disturb the wurtzite crystal structure of parent ZnO. It is clearly seen that the FWHM of the reflection peaks decreased after adding the dopant cations, indicating growth of the crystallinity or changes in the crystal strains [9]. Also a negligible shift in peaks is observed for which FWHM obviously decreased when doped with different La and La+Ag concentration compared to un-doped ZnO nanoparticles. The significant change in position of peaks is attributed to the different ionic radii of Zinc, Lathanum and silver ($Zn^{2+} \sim 0.074$ Å, $La^{3+} \sim 0.103$ Å and $Ag^+ \sim 0.115$ Å). The shifting of the XRD peaks with the doped and co-doped ZnO suggests the substitution of Zn^{2+} by La and Ag in the ZnO host lattice. The similar shift has been reported in transition metal doped ZnO nanostructures by Ekambaram et al. [10] and Dinesha et al. [11]. Wurtzite lattice parameters such as the values of d, the distance between adjacent planes in the Miller indices (hkl), lattice constants «a» and «c» are calculated from the peak positions of the XRD data and are summarized in (Table 1).

It is seen from Table 1 that the lattice constant values of the ZnO increase with the substitution of La and Ag. The trend can be explained on the basis of the ionic radii of the constituent ions. The La^{3+} and Ag^+ ions replace Zn^{2+} ions. This makes the lattice to expand and lattice parameter increase since radii of La^{3+} ion (0.103 nm)

and Ag^+ ion (0.115 nm) is bigger than that of Zn^{2+} ion (0.064 nm) [12–14].

The XRD can be utilized to evaluate peak broadening with crystallite size and lattice strain due to dislocation. The crystalline size of the un-doped ZnO and La doped ZnO and La+Ag codoped ZnO with different concentration were determined by the X-ray line broadening method using the Debye-Scherer s equation as

$$ D = \frac{0.9\lambda}{\beta \cos\theta} , $$

where D is the crystalline size in nanometers, λ is the wavelength of the radiation (1.542 Å), β is the peak width at half maximum intensity, and q is the peak position. Crystallite size of pure and doped ZnO is found to be in the range of 10–20 nm.

It is supposed that with decreasing particle size, the number of ZnO nanoparticles per unit volume of the powder increases resulting in increased surface area. X-ray diffraction results clearly indicate that increase in lanthanum and silver content results in decrease of zinc oxide grain size. It can be assumed that with decreasing particle size, the number of particles per unit volume of powder increases resulting in increased surface area [15].

3.2 Morphological studies

Fig. 2 (a, b and c) represent SEM micrographs of pure, La doped and La+Ag codoped ZnO nanoparticles. From micrographs, it is clear that uniformly distributed hexago-

Table 1. Structural parameters of pure, La doped and La+Ag co-doped ZnO nanoparticles.

Samples	Molarity variation	Lattice parameter (Å)			Volume (Å) x 10³	Dislocation density, δ x 10¹⁵(lines/m²)	Grain size (D) nm	Strain (ε), x 10⁻³
		a	*c*	*c/a*				
ZnO		3.236	5.182	1.601	47.010	2.992	18.317	1.896
ZnO(La)	0.1M	3.280	5.208	1.587	45.856	6.386	12.514	2.987
ZnO(La)	0.2M	3.265	5.236	1.641	48.348	4.046	15.720	2.209
ZnO(La)	0.3M	3.246	5.328	1.642	49.387	3.820	16.167	2.144
ZnO(Ag+La)	0.1M	3.340	5.164	1.545	49.758	3.377	17.209	2.014
ZnO(Ag+La)	0.2M	3.414	5.184	1.518	52.569	5.724	13.217	2.623
ZnO(Ag+La)	0.3M	3.453	5.180	1.500	53.612	5.495	13.419	2.568
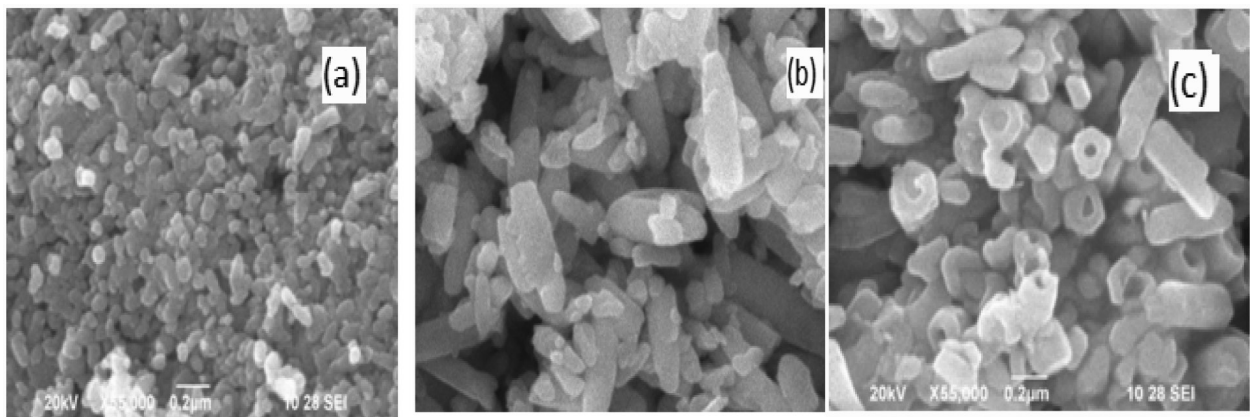
Figure 2. (*a*) SEM images of pure ZnO, (*b*) La doped and (*c*) La+Ag co-doped ZnO nanoparticles.
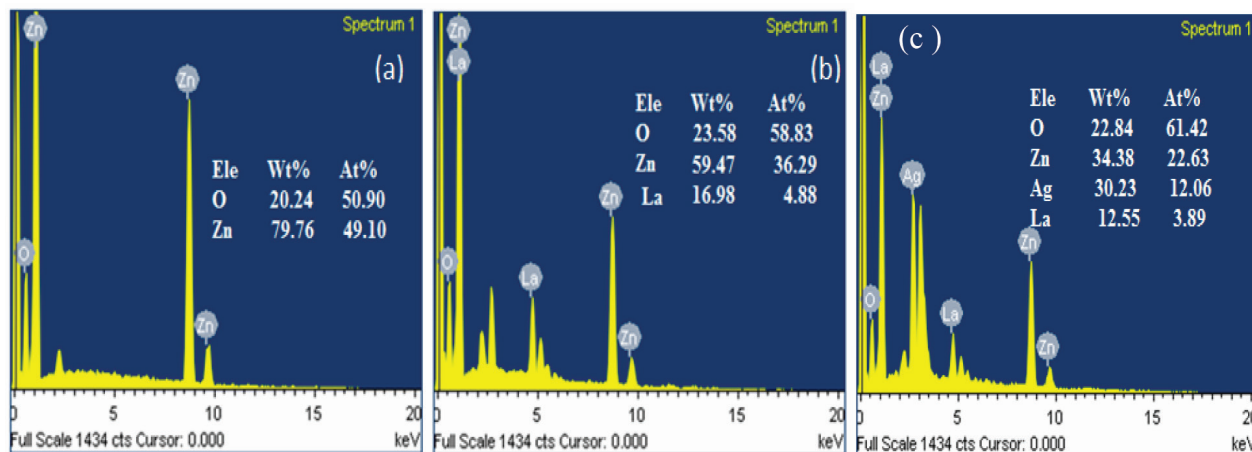
Figure 3. (*a*) EDAX images of pure ZnO, (*b*) La doped and (*c*) La+Ag co-doped ZnO nanoparticles.

nal shaped and rod shaped particles were observed for the pure and doped ZnO nanoparticles. The particle size is decreased for doped ZnO nanocrystals. The morphological observation of SEM results indicates particles with less aggregation can be obtained from this method.

EDAX analysis is used to examine the elemental compositions such as Zn, La, Ag and O in the prepared samples. Fig. 3 (*a*, *b* and *c*) shows the EDAX spectra of pure ZnO, doped with La and co-doped with La+Ag. In EDAX spectrum, the peaks were evident related to Zn, O, La and Ag which clearly support that nanoparticles are made of Zn, O, La and Ag. No other peaks related to impurities were detected in the spectrum which further confirms the purity of the compounds. The presence of La and Ag with appropriate weight percentage in Zn–La–O and Zn–La–Ag–O and chemical purity of the samples is confirmed by EDAX analysis and is tabulated in (Table 2).

Table 2. The weight percentage and atomic percentage of pure, La doped and La+Ag co-doped ZnO nanoparticles.

Samples	Elements	Weight percentage	Atomic percentage
ZnO	Zn	79.76	49.10
	O	20.24	50.90
ZnO+La	Zn	59.47	36.29
	O	23.58	58.83
	La	16.98	4.88
ZnO+(La+Ag)	Zn	34.38	22.63
	O	22.84	61.42
	La	12.55	3.89
	Ag	30.23	12.06

3.4 FTIR Studies

FTIR is one of the most widely used techniques for the detection of the functional groups and quality of the material in pure compounds and mixtures. The FTIR spectra of pure, La doped and La+Ag co-doped recorded in the range 400–4000 cm^{-1} is as shown in Fig. 4. The spectra shows the Zn–O bond appear at around 563 cm^{-1} which may be related with oxygen vacancy or oxygen deficiency in ZnO [16, 17]. This oxygen deficiency
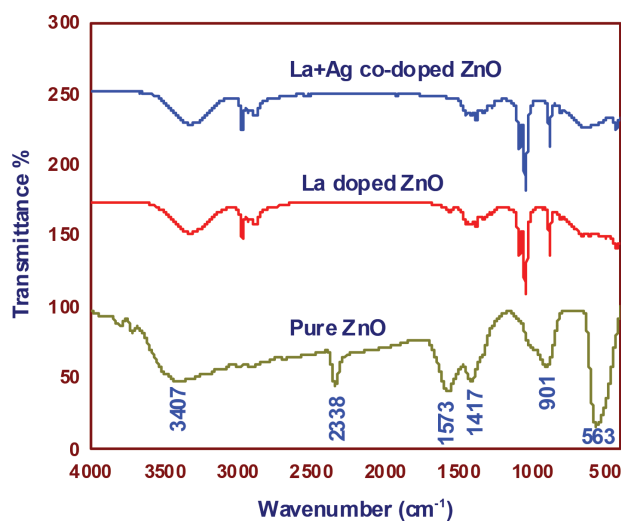
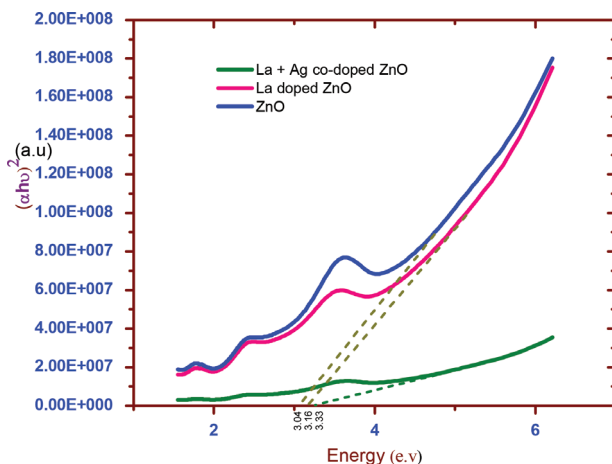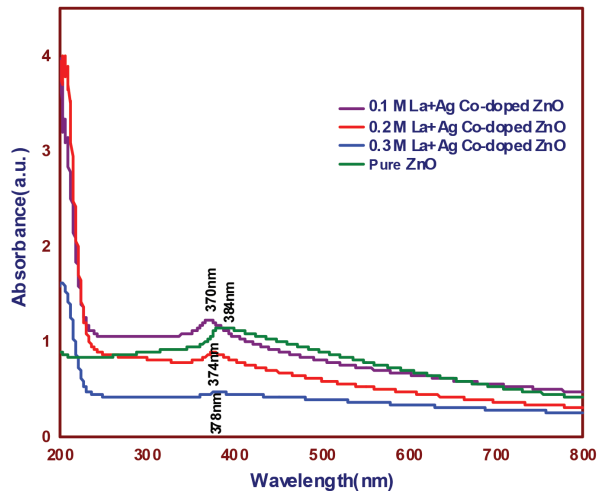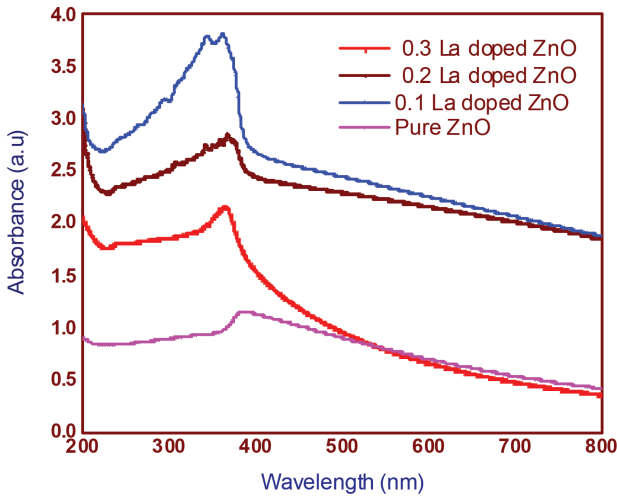**Figure 4.** FTIR images of pure, La doped and La+Ag co-doped ZnO nanoparticles.

should translate into an enhanced green emission in UV absorption spectra [18]. The broad peak around 3407 cm^{-1} is assigned to the O–H stretching vibration of water molecule [19, 20]. A weak absorption peak at 2338 cm^{-1} is ascertained due to the –CH$_2$ asymmetric stretching vibration present in the precipitating agent [21]. The peaks at 1417 cm^{-1} correspond to the C–O absorption of ZnO surface and bands at 901 cm^{-1} correspond to C–O stretching vibrations. These results further confirm the formation of Wurtzite structure in nanoparticles synthesized at room temperature.

3.5 Optical Studies

Optical properties of ZnO particles become important as the size of the particles are reduced to nano size. UV-Visible absorption spectroscopy is an efficient technique to monitor the optical properties of quantum-sized ZnO nano particles. To study the effect of the doping of Lanthanum and silver on the absorption of ZnO, we measured the absorption spectra of the samples at the room temperature as shown in Fig. 5 (*a* and *b*) For pure ZnO nano particles,

the absorption intensity decreases for wavelength greater than 384 nm. This was assigned to the intrinsic band gap of the ZnO due to electron transitions from the valence band to the conduction band. After being doped with La and co-doped with La+Ag, the absorption peaks shifted towards shorter wavelength region from 384 nm i.e. blue shifted. The blue shift in the absorption spectrum edge is

a clear indication for the incorporation of La and La+Ag inside the ZnO lattice [22, 23]. It is apparent that the absorbtion edge shifts to higher energy or lower wavelengths with decreasing the size of ZnO nanoparticles i.e the size of the particles starts decreasingdue to percentage increase in doping. This marked shift is due to quantum confinement effect [24]. The bandgap energy is evaluated for the samples using the relation,
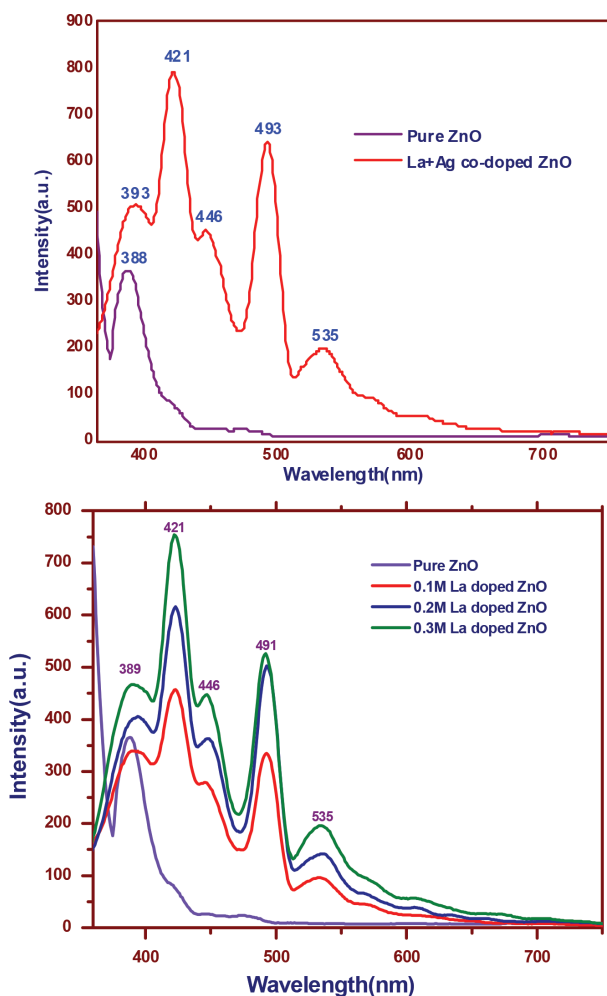
$$(\alpha h v) = A\left(h v - E_g\right)^n,$$

where α is the absorption coefficient, A is a constant, $h v$ is the incident photon energy, E_g is the energy band gap of the material. The value of n is 1/2 or 2 depending upon whether the transition from valence band to conduction band is direct or indirect. Taucplot Fig. 5c is drawn of $(\alpha h v)^2$ vs $h v$. The extrapolation of the liner part that meets the abscissa gives the value of the band gap energy E_g of the material which is listed in the Table 3. The band gap energy estimated for all the samples pure (ZnO) at 600 °C is 381 nm that is slightly higher, and for further increase in doped Molarity the band gap decreases.

Table 3. The band gap energy values of pure, La doped and La+Ag co-doped ZnO nanoparticles.

Sample	Energy gap (E_g)
ZnO	3.33
La Doped ZnO	3.16
La+Ag codoped ZnO	3.04

The PL spectra are useful to disclose the efficiency of charge carrier trapping, immigration, and transfer and to understand the fate of electron hole pairs in semiconductor particles since PL emission results from the recombination of free carrier. PL spectra of pure, La doped and La+Ag co-doped ZnO nanoparticles is taken and is as shown in Fig. 6 (*a* and *b*). The luminescence peak of pure ZnO observed at 388 nm and for La doped at 421 and 493 nm, for co-doped ZnO observed at 421 and 491 nm, there is substantial enhancement of luminescence intensity due to increase of La and La+Ag concentration, which acts as effective luminescent centers. The PL results show that co-doped rare earth elements are the major luminescent component and can effectively improve the luminescence of La doped and La+Ag co-doped ZnO. A weak ultraviolet (UV) emission at 490 nm is observed for pure ZnO nanoparticles and is related to the near band- edge emission [25–27]. Three weak and two strong emissions at 393, 446, 535 nm and 421, 493 nm were observed for the La doped ZnO nanoparticles which have also been observed for La+Ag co-doped ZnO nano particles. Compared with the PL spectrum of pure ZnO, the UV- emission peak of La doped ZnO and La+Ag co-doped samples exhibit a considerable redshift.

Figure 5. Optical absorption spectra of pure and (*a*) La doped ZnO nanoparticles, (*b*) La+Ag co-doped ZnO, (*c*) $(\alpha h v)^2$ vs ($h v$) spectra of doped and co-doped ZnO nanoparticles.

Figure 6. Photo Luminescense spectra of pure and (*a*) La doped ZnO nanoparticles, (*b*) La+Ag co-doped ZnO nanoparticles.

4. Conclusion

In the present study, pure, La doped and La+Ag co-doped ZnO nanoparticles were synthesised via Sol Gel route and further analyzed through X-ray diffraction, scanning electron microscopy, Energy Dispersive X-ray Absorption (EDAX), Fourier transform infrared spectroscopy (FTIR), UV-Vis absorbtion spectroscopy, and Photo Luminescence (PL) Characterization. The XRD spectrum demonstrates that nanoparticles have the hexagonal wurtzite structure. The nano particles of average size 10–20 nm have been obtained at various concentration of La and La+Ag through sol-gel method. The substitution of La and co- substitution of La+Ag does not disturb the wurtzite crystal structure of parent ZnO. SEM images showed the uniformly distributed hexagonal shaped and rod shaped particles were observed for the pure and doped ZnO nanoparticles. FTIR showed that various functional groups are present in pure and La doped ZnO nanoparticles.Optoelectronic investigation has been carried out by UV-Vis spectroscopy and Photoluminescence. UV visible absorption spectra results of La doped and La+Ag co-doped ZnO nanoparticles indicates that there is a blue shift in absorption spectra. The band gap energy estimated for all the samples pure (ZnO) at 600 °C is 381 nm that is slightly higher, and for further increase in calcinations temperature the band gap decrease. Photoluminescence spectra results that pure ZnO nanoparticles exhibits UV emission peak at 388 nm observed in the UV and in the visible region. Thus, the overall results show that the co-doped (La+Ag) ZnO nanostructures are suitable for the development of optoelectronic and spintronics devices.

References

1. Jungnickel V., Henneberger F. Luminescence related processes in semiconductor nanocrystals –The strong confinement regime. *J. Luminescence*, 1996; 70(1–6): 238–252. https://doi.org/10.1016/0022-2313(96)00058-0

2. Chunming Jin, Jiaqi Yu, Lingdong Sun, Kai Dou, Shanggong Hou, Jialong Zhao, Yimin Chen, Shihua Huang. Luminescence of Mn^{2+} doped ZnS nanocrystallites. *J. Luminescence*, 1995; 66–67: 315–318. https://doi.org/10.1016/0022-2313(95)00160-3

3. Chamarro M., Gaurdon C., Lavallard P. Photoluminescence polarization of semiconductor nanocrystals. *J. Luminescence*, 1996; 70(1–6): 222–237. https://doi.org/10.1016/0022-2313(96)00057-9

4. Sathya B., Benny Anburaj D., Porkalai V., Nedunchezhian G. Raman scattering and photoluminescence properties of Ag doped ZnO nano particles synthesized by sol-gel method. *J. Mater. Sci.: Mater. Electron.*, 2017; 28(8): 6022–6032. https://doi.org/10.1007/s10854-016-6278-3

5. Ping Ping Yang, Mengkai Lü, Guangjun Zhou, DuoRong Yuan, Dong Xu. Photoluminescence characteristics of ZnS nanocrystallites co-doped with Co^{2+} and Cu^{2+}. *Inorganic Chemistry Comm.*, 2001; 4(12): 734–737. https://doi.org/10.1016/S1387-7003(01)00322-7

6. Kulkarni S.S., Shirsat M.D. Optical and structural properties of zinc oxide nanoparticles. *Int. J. Advanced Research in Physical Science*, 2015; 2(1): 14–18. https://www.arcjournals.org/pdfs/ijarps/v2-i1/3.pdf

7. Gabás M., Landa-Cánovas A., Costa-Krämer J. L., Agulló-Rueda F., González-Elipe A. R., Díaz-Carrasco P., Hernández-Moro J., Lorite I., Herrero P., Castillero P., Barranco A., Ramos-Barrado J.R. Differences in n-type doping efficiency between Al- and Ga-ZnO films. *J. Appl. Phys.*, 2013; 113(16): 163709. https://doi.org/10.1063/1.4803063

8. Al-Kuhaili M.F., Durrani S.M.A., El-Said A.S., Heller R. Influence of iron doping on the structural, chemical, and optoelectronic properties of sputtered zinc oxide thin films. *J. Materials Research*, 2016; 31(20): 3230–3239. https://doi.org/10.1557/jmr.2016.343

9. Neha Sharma, Jitender Kumar, Shaveta Thakur, Shruti Sharma, Vikas Shrivastava. Antibacterial study of silver doped zinc oxide nanoparticles against Staphylococcus aureus and Bacillus subtilis. *Drug Invention Today*, 2013; 5(1): 50–54. https://doi.org/10.1016/j.dit.2013.03.007

10. Ekambaram S., Iikubo Y., Kudo A. Combustion synthesis and photocatalytic properties of transition metal-incorporated ZnO. *J. Alloys Compd.*, 2007; 433(1–2): 237–240. https://doi.org/10.1016/j.jallcom.2006.06.045

11. Dinesha M.L., Prasanna G.D, Naveen C.S, Jayanna H.S. Structural and dielectric properties of Fe doped ZnO nanoparticles. *Indian J. Phys.*, 2013, 87(2): 147–153. https://doi.org/10.1007/s12648-012-0182-3

12. Ganure K.A., A. Dhale L.A., T. Katkam V.T., Lohar K.S. Synthesis and characterization of lanthanum-doped Ni-Co-Zn spinel ferrites nanoparticles via normal micro- emulsion method. *Int. J. Nanotechnology and Applications*, 2017; 11(2): 189–195.

13. Lijun Zhao, Hua Yang, Lianxiang Yu, Wei Sun, Yuming Cui, Yu Yan, Shouhua Feng. Structure and magnetic properties of $Ni_{0.7}Mn_{0.3}Fe_2O_4$ nanoparticles doped with La_2O_3 *Phys. Status Solidi (a)*, 2004; 201(14): 3121–3128. https://doi.org/10.1002/pssa.200406856

14. CRC Handbook of Chemistry and Physics, 86th Edition. Ed. by D.R. Lide. Boca Raton (FL): CRC Press, 2005: 2544.

15. Becheri A., Dürr M., Lo Nostro P., Baglioni P. Synthesis and characterization of zinc oxide nanoparticles: application to textiles as UV-absorbers. *J. Nanopart. Res.*, 2008; 10(4): 679–689. https://doi.org/10.1007/s11051-007-9318-3

16. Rashmi R., Devi Tarun K. Maji. Effect of nano-ZnO on thermal, mechanical, UV stability, and other physical properties of wood polymer composites. *Industrial & Engineering Chemistry Research*, 2012; 51(10): 3870–3880. https://doi.org/10.1021/ie2018383

17. Nedunchezhian G., Benny Anburaj D., Gokulakumar B., Johnson Jeyakumar S. Microwave synthesis of Au/Ag doped nano Hydroyapatite from deal Mussel shell. *Int. J. Adv. Sci. Eng.*, 2017; 3(3): 353–356. http://mahendrapublications.com/Document/MP242436_Manuscript_2018_02_16_0248.pdf

18. Thangeeswari T., Ann Tresa George, Arun Kumar A. Optical properties and FTIR studies of cobalt doped ZnO nanoparticles by simple solution method. *Indian J. Science and Technology*, 2016; 9(1): 1–4. https://doi.org/10.17485/ijst/2016/v9i1/85776

19. Wahab R., Ansari S.G., Kim Y.S., Seo H.K., Kim G.S., Khang G., Shin H.-S. Low temperature solution synthesis and characterization of ZnO nano-flowers. *Materials Research Bulletin*, 2007; 42(9): 1640–1648. https://doi.org/10.1016/j.materresbull.2006.11.035

20. Porkalai V., Benny Anburaj D., Sathya B., Nedunchezhian G., Meenambika R. Study on the synthesis structural optical and electrical properties of ZnO and lanthanum doped ZnO nano particles by sol-gel method. *Mechanics, Materials Science and Engineering Journal, Magnolithe*, 2017; 9. https://doi.org/10.4028/www.scientific.net/NHC.17.101

21. Costenaro D., Carniato F., Gatti G., Bisio C., Marchese L. On the physico-chemical properties of ZnO nanosheets modified with luminescent CdTe nanocrystals. *J. Phys. Chem. C*, 2011; 115(51): 25257–25265. https://doi.org/10.1021/jp209267s

22. Radovanovic P.V., Norberg N.S., McNally K.E., Gamelin D.R. Colloidal transition- metal-doped ZnO quantum dot. *J. Am. Chem. Soc.*, 2002; 124(51): 15192–15193. https://doi.org/10.1021/ja028416v

23. Varghese N., Panchakarla L.S., Hanapi M., Govindaraj A., Rao C.N.R. Solvothermal synthesis of nanorods of ZnO, N-doped ZnO and CdO. *Materials Research Bulletin*, 2007; 42(12): 2117–2124. https://doi.org/10.1016/j.materresbull.2007.01.017

24. Porkalai V., Benny Anburaj D., Sathya B., Nedunchezhian G., Meenambika R. Effect of calcinations on the structure and morphological properties of Ag and In co-doped ZnO nanoparticles. *J. Mater. Sci.: Mater. Electron.*, 2017; 28(3): 2521–2528. https://doi.org/10.1007/s10854-016-5826-1

25. Rana S.B., Singh A., Singh S. Characterisation and optical studies of pure and Sb doped ZnO nanoparticles. *Int. J. Nanoelectronics and Materials*, 2013; 6: 45–57.

26. Viswanatha R., Sapra S., Gupta S.S., Satpati B., Satyam P.V., Dev B.N., Sarma D.D. Synthesis and characterization of Mn-doped ZnO nanocrystals. *J. Phys. Chem. B*, 2004; 108(20): 6303–6310. https://doi.org/10.1021/jp049960o

27. Punithavathy I.K., Richard J.P., Jeyakumar S.J., Jothibas M., Praveen P. Photodegradation of methyl violet dye using ZnO nanorods. *J. Mater. Sci.: Mater. Electron.*, 2017; 28(3): 2494–2501. https://doi.org/10.1007/s10854-016-5823-4